

# Measurement of the Spatial Correlation Function of Phase Fluctuating Bose-Einstein Condensates

D. Hellweg,<sup>\*</sup> L. Cacciapiuoti, M. Kottke, T. Schulte, K. Sengstock<sup>1</sup>, W. Ertmer, and J.J. Arlt

*Institut für Quantenoptik, Universität Hannover, Welfengarten 1, 30167 Hannover, Germany*

<sup>1</sup>*Institut für Laserphysik, Universität Hamburg, Jungiusstraße 2, 20355 Hamburg, Germany*

(Dated: October 24, 2018)

We measure the intensity correlation function of two interfering spatially displaced copies of a phase fluctuating Bose-Einstein Condensate (BEC). It is shown that this corresponds to a measurement of the phase correlation properties of the initial condensate. Analogous to the method used in the stellar interferometer experiment of Hanbury Brown and Twiss, we use spatial intensity correlations to determine the phase coherence lengths of elongated BECs. We find good agreement with our prediction of the correlation function and confirm the expected coherence length.

PACS numbers: 03.75.Hh, 03.75.Nt, 39.20.+q

Since the first realization of Bose-Einstein condensation in dilute atomic gases their coherence properties have attracted considerable theoretical and experimental interest. This interest is due to the central role of the coherence properties for the theoretical description and conceptual understanding of BECs and their use as a source of coherent matter waves in many promising applications.

Remarkable measurements demonstrated the phase coherence of three-dimensional (3D) condensates well below the BEC transition temperature  $T_c$  [1, 2, 3] and even at finite temperature [4]. However, low dimensional systems show a qualitatively different behavior. In particular, it has been predicted that one-dimensional and even very elongated, three-dimensional BECs exhibit strong spatial and temporal fluctuations of the phase while fluctuations in their density distribution are suppressed [5, 6]. Thus, the coherence properties are significantly altered, resulting in a reduced coherence length which can be much smaller than the condensate length. In this case the degenerate sample is called a quasicondensate. This regime has been subject of recent theoretical efforts based on the Bogoliubov [7] and Popov [8, 9] theory to extend and generalize the description of BEC and to calculate correlation functions [10]. The phase fluctuations are caused by thermal excitations of low energy axial modes and thus depend strongly on the temperature and trapping geometry. In particular, for very elongated BECs a nearly phase coherent sample can only be achieved far below  $T_c$ . Phase fluctuations were first observed using the formation of density modulations during ballistic expansion of a condensate [11, 12, 13]. In addition, their effect on the momentum distribution has been demonstrated using Bragg spectroscopy [14, 15]. Nonequilibrium properties of these condensates have been studied using a condensate focussing technique [16].

In this Letter we report on a direct measurement of the spatial correlation function of phase fluctuating BECs. To measure the phase correlation properties we interfere two copies of a BEC with a spatial displacement

$d$  (Fig. 1). The measured interference pattern is determined by the phase pattern of the original condensate and a global phase difference between the two copies introduced by the interferometer. By varying the displacement  $d$  the first order correlation function can, in principle, be measured. However, this method is very sensitive to fluctuations in the global phase difference and the measurement is further complicated by the statistical nature of phase fluctuations. We show that the use of intensity correlations in the interference pattern overcomes these problems and provides the desired information about the phase correlations in the initial condensate. The result of this measurement is described by the spatial second order correlation function and yields the phase coherence length of the BEC. In many respects our measurement is closely related to the stellar interferometer of Hanbury Brown and Twiss [17, 18]. They measured the intensity of starlight falling onto two detectors and computed the intensity correlations electronically as a function of the detectors' distance. This measurement yields the transverse coherence length of the stellar light and allowed them to determine the stars' diameter. Unlike the Michelson stellar interferometer, which uses first order correlations, atmospheric fluctuations do not disturb this measurement. In the same way, global phase fluctuations in the interferometer setup do not disturb our measurement.

Our experiments were performed with  $^{87}\text{Rb}$  Bose-Einstein condensates in the  $|F=1, m_F=-1\rangle$  hyperfine ground state. Further details of our experimental apparatus were described previously [12]. The confining potential was provided by a cloverleaf type magnetic trap with an axial trapping frequency of  $\omega_x = 2\pi \times 3.4 \text{ Hz}$  and a radial frequency adjusted between  $\omega_r = 2\pi \times 300 \text{ Hz}$  and  $\omega_r = 2\pi \times 380 \text{ Hz}$ . The number of condensed atoms  $N_0$  was varied between  $4 \times 10^4$  and  $6 \times 10^5$ . To allow the system to reach an equilibrium state we typically waited for 4s after obtaining BEC by evaporative cooling (with rf "shielding") [25]. The interferometric scheme is shown in Fig. 1 and is based on two  $\pi/2$  Bragg diffrac-

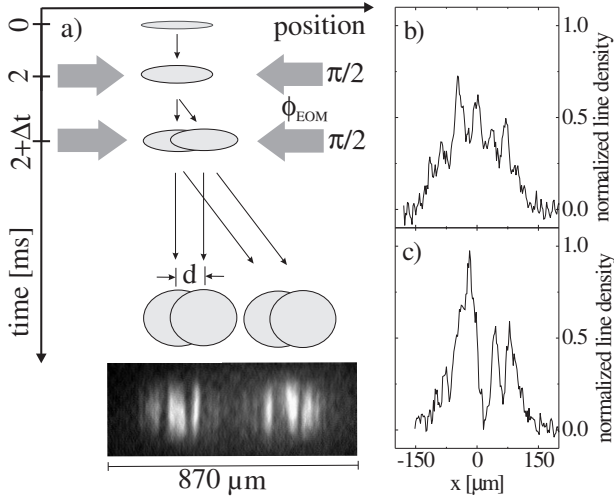


FIG. 1: (a) The interferometer is realized by two  $\pi/2$  Bragg diffraction pulses. We apply the first pulse after a ballistic expansion time of 2 ms to reduce mean-field effects and atomic scattering. The spatial displacement  $d$  is determined by the time  $\Delta t$  between the pulses. Typical line density profiles are shown for a phase coherence length of  $L_\phi \approx 25 \mu\text{m}$  with  $d = 7 \mu\text{m}$  (b) and  $d = 35 \mu\text{m}$  (c). Only one of the two output ports is displayed.

tion pulses. These pulses were produced by two counterpropagating laser beams with a frequency difference set to the two-photon resonance. They were detuned by about 3 GHz from the atomic resonance to suppress spontaneous emission. The pulse duration of  $100 \mu\text{s}$  was chosen long enough to avoid higher order diffraction and sufficiently short to avoid any sensitivity to the internal velocity distribution of the phase fluctuating BECs. After a time-of-flight of 30 to 40 ms the two output ports spatially separate and the atoms were detected by resonant absorption imaging. We integrate the absorption images along the radial direction of the condensate and subtract the thermal background to obtain line density profiles.

Typical measured line density profiles are shown in Fig. 1. These profiles provide a qualitative argument for the use of intensity correlations as a particularly useful tool for our measurements. When the displacement  $d$  between the overlapping clouds is chosen smaller than the phase coherence length in the sample (Fig. 1b) regions with almost identical phases are brought to overlap and the resulting interference signal is rather smooth. If however  $d$  is larger than the phase coherence length, regions with substantially different phases overlap, resulting in an irregular but high contrast interference signal (Fig. 1c). In both cases an average over many realizations and relative phases results in the same smooth profile in the two output ports of the interferometer, revealing no information about the coherence properties. Nonetheless Fig. 1c clearly contains information about the spa-

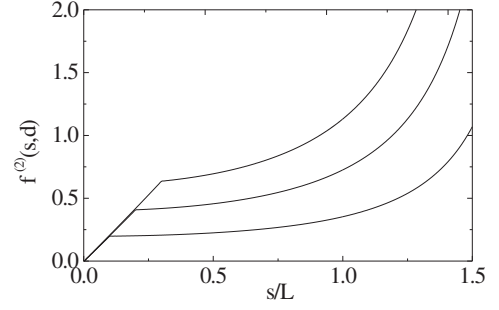


FIG. 2: Numerical computation of the function  $f^{(2)}(s, d) \equiv f^{(2)}(\frac{s-d}{2}, \frac{s+d}{2}, \frac{s-d}{2}, \frac{s+d}{2})$  for three different  $d$ . From top to bottom:  $d/L = 0.3, 0.2, 0.1$ . The particular choice of positions corresponds to the experimentally relevant case.

tial coherence properties. An appropriate analysis of the correlations in the density profile yields an intensity correlation function that does not vanish in an averaging process and contains the desired information about the coherence properties.

We therefore start our analysis by calculating the spatial second order correlation function for the case of phase fluctuating BECs. In its most general definition [19] it is given by

$$g^{(2)}(x_1, x_2, x_3, x_4) = \frac{\langle \hat{\psi}^\dagger(x_1) \hat{\psi}^\dagger(x_2) \hat{\psi}(x_3) \hat{\psi}(x_4) \rangle_T}{\sqrt{\prod_{i=1}^4 \langle \hat{\psi}^\dagger(x_i) \hat{\psi}(x_i) \rangle_T}}, \quad (1)$$

where  $\langle \dots \rangle_T$  denotes an average over an ensemble at thermal equilibrium at temperature  $T$ . It contains the spatial intensity correlation function  $g^{(2)}(x_1, x_2) = g^{(2)}(x_1, x_2, x_2, x_1)$  as a special case. For 3D condensates with repulsive interactions in elongated trapping potentials density fluctuations are suppressed by the mean-field potential [6, 13, 14]. Therefore the total field operator of the condensed atoms can be written as  $\hat{\psi}(x) = \sqrt{n_0(x)} \exp(i\hat{\phi}(x))$ , where  $\hat{\phi}(x)$  is the operator of the phase [6] and  $n_0(x)$  is the density in the Thomas-Fermi approximation. For this field operator one can show that all higher order correlation functions can be expressed as products of the first order correlation function [20]. Using the explicit expression of the phase operator given by Petrov et al. [6] we obtain the second order correlation function:

$$g^{(2)}(x_1, x_2, x_3, x_4) = \exp \left[ -\frac{1}{2l_\phi} f^{(2)}(x_1, x_2, x_3, x_4) \right], \quad (2)$$

with

$$f^{(2)}(x_1, x_2, x_3, x_4) = \frac{1}{8} \sum_j \frac{(j+2)(2j+3)}{j(j+3)(j+1)} \left[ P_j^{(1,1)} \left( \frac{x_1}{L} \right) + P_j^{(1,1)} \left( \frac{x_2}{L} \right) - P_j^{(1,1)} \left( \frac{x_3}{L} \right) - P_j^{(1,1)} \left( \frac{x_4}{L} \right) \right]^2, \quad (3)$$

where  $P_j^{(1,1)}$  are Jacobi polynomials,  $j$  is a positive integer,  $2L$  is the condensate length and

$$l_\phi = \frac{L_\phi}{L} = \frac{15N_0(\hbar\omega_x)^2}{32\mu k_B T} \quad (4)$$

is the phase coherence length in the condensate center (in units of  $L$ ). Here  $\mu$  denotes the chemical potential and  $k_B$  the Boltzmann constant. The function  $f^{(2)}$  is shown in Fig. 2 and contains the functional form of phase fluctuations in elongated condensates. All experimental parameters are contained in the phase coherence length  $l_\phi$ .

Let us demonstrate how the interferometric sequence described above can be used to measure  $g^{(2)}$ . In each output port of the interferometer the superposition of two ballistically expanded spatially displaced copies of the original wave function is produced. The field operator of the atoms in one output port can be expressed as

$$\hat{\psi}_f(x, d) = \frac{1}{2} \{ \sqrt{n(x-d/2)} e^{i\hat{\phi}^+(x-d/2)} + \sqrt{n(x+d/2)} e^{i\hat{\phi}^-(x+d/2)} e^{i\phi_{\text{rel}}} \}, \quad (5)$$

with  $\hat{\phi}^\pm(x) = \hat{\phi}(x) \pm \beta x + \alpha x^2$  [26]. The linear term results from the mean-field repulsion between the copies of the condensate [21] and the quadratic term originates from the self-similar expansion [22, 23]. The self-similar expanded density distribution  $n(x)$  differs only slightly from the initial distribution because the increase of axial size during expansion is small for very elongated condensates (about 1% for our experimental conditions). The relative global phase between the two overlapping clouds  $\phi_{\text{rel}} = \delta_{12}\Delta t + \delta\phi_{\text{eff}}$  is determined by the Bragg diffraction process, where  $\delta\phi_{\text{eff}}$  is the change in the relative phase of the Bragg beams between the two pulses and  $\delta_{12}$  is the detuning from the two-photon resonance. In our experiment  $\delta\phi_{\text{eff}}$  can be controlled by using an electro-optical modulator [24],  $\delta_{12}$  depends on the frequency difference of the Bragg beams and the axial release velocity of the condensate. Note that even a small change in the release velocity of  $0.033 \mu\text{m/ms}$  leads to a phase change of  $\pi/2$  for a time  $\Delta t = 3 \text{ ms}$  between the Bragg pulses [27]. The insensitivity to such randomly varying global phases is a major advantage of the intensity correlation method.

In analogy to the definition of the correlation coefficient we define a normalized intensity correlation function

$$\gamma_f^{(2)}(x_1, x_2, d) = \frac{\langle (\hat{I}_1 - \langle \hat{I}_1 \rangle)(\hat{I}_2 - \langle \hat{I}_2 \rangle) \rangle}{\sqrt{\langle (\hat{I}_1 - \langle \hat{I}_1 \rangle)^2 \rangle} \sqrt{\langle (\hat{I}_2 - \langle \hat{I}_2 \rangle)^2 \rangle}}, \quad (6)$$

with the intensity operator  $\hat{I}_{1,2} = \hat{\psi}_f^\dagger(x_{1,2}, d)\hat{\psi}_f(x_{1,2}, d)$ . Here the averages are taken over an ensemble in thermal equilibrium and over all relative phases. The possible values of  $\gamma_f^{(2)}$  range between +1 (perfect correlation) and

-1 (perfect anticorrelation); if  $\hat{I}_1$  and  $\hat{I}_2$  are uncorrelated  $\gamma_f^{(2)} = 0$ . By substituting Eq. (5) into Eq. (6) we obtain

$$\gamma_f^{(2)}(x_1, x_2, d) = \cos[2(x_1 - x_2)(\alpha d - \beta)] \times \exp \left[ -\frac{1}{2l_\phi} f^{(2)}(x_1 - \frac{d}{2}, x_2 + \frac{d}{2}, x_2 - \frac{d}{2}, x_1 + \frac{d}{2}) \right]. \quad (7)$$

The normalized intensity correlation function is the product of two contributions. A cosine resulting from the self-similar expansion and mean-field repulsion and an exponentially decaying term containing the influence of the phase fluctuations. The decay constant of this function is the phase coherence length. Comparison with Eq. (2) shows that a measurement of  $\gamma_f^{(2)}$  is equivalent to a measurement of the second order correlation function of the trapped condensate.

The measurement of  $\gamma_f^{(2)}$  is performed in the following way: For a given trap configuration, evaporative cooling ramp and fixed displacement  $d$ , a series of measurements is recorded by scanning the relative phase of the Bragg beams with the electro-optical modulator in small steps between 0 and  $2\pi$ . This insures that the global phase  $\phi_{\text{rel}}$  contains all values with equal probability. We experimentally determine  $\gamma_f^{(2)}$  analogous to Eq. (6). The ensemble averages  $\langle \hat{I}(x) \rangle$  are obtained by averaging all interference patterns  $I(x)$  recorded in a series. Then the quantity  $I(x) - \langle \hat{I}(x) \rangle$  can be determined for each realization. The average of these values according to Eq. (6) yields  $\gamma_f^{(2)}$ . To simplify the analysis we evaluate  $\gamma_f^{(2)}$  at symmetric positions around the center of the interference pattern such that  $x_1 = -x_2 = s/2$ . Then  $\gamma_f^{(2)}(s, d) = \gamma_f^{(2)}(-s/2, s/2, d)$  can be expressed as a function of  $s$  for a given displacement  $d$ . Typical results are shown in Fig. 3, clearly displaying the functional form of a damped cosine.

To extract quantitative results we fit the measured function with the theoretical one given in Eq. (7). The fit contains only  $l_\phi$  and the frequency of the cosine as free parameters. Figure 3 compares measured correlation functions with the corresponding fits, confirming the excellent agreement with the expected functional form. Although the phase coherence length also depends on the trapping potential and the temperature, the data sets shown in Fig. 3 differ mainly due to the number of condensed atoms, which was set to  $4.4 \times 10^4$  (●),  $2.9 \times 10^5$  (+) and  $5.0 \times 10^5$  (□). Except for the smallest atom number a minimum is clearly visible and unambiguously defines the frequency of the cosine [28]. The damping of this oscillation yields the phase coherence length. As expected (see Eq. (4)), the damping is stronger for small  $N_0$ . In case of the smallest  $N_0$  no oscillation is visible, indicating a significant decrease of the phase coherence length.

We have performed such measurements for a large variety of atom numbers and temperatures. The good agreement between the measured phase coherence length ob-

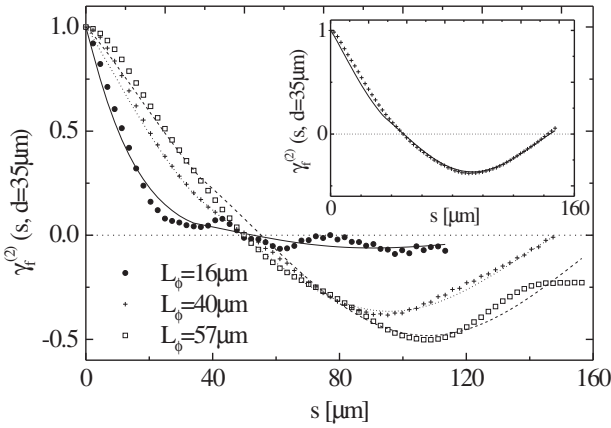


FIG. 3: Measured correlation functions (points) compared to fitted theoretical curves (lines). Each measured function is based on  $\approx 25$  realizations and plotted up to  $s = 0.8L$ . Neighboring points are not independent since they are based on a common set of experimental realizations. Inset: Numerical simulation including the phase and density evolution (points) and the analytical function Eq. (7) (line), both for the parameters of the  $L_\phi = 40 \mu\text{m}$  curve.

tained from the fit and the theoretically predicted one is shown in Fig. 4. By varying the displacement  $d$  we have confirmed that the measured phase coherence lengths are independent of this parameter. In all cases the phase coherence length was much smaller than the condensate length, which ranged from  $280 \mu\text{m}$  up to  $420 \mu\text{m}$ , i.e. our measurements were performed in the quasicondensate regime.

So far we have neglected the evolution of the phase fluctuations during ballistic expansion. This evolution leads to a change of the original phase pattern and the appearance of density modulations. Using the full evolution of the wave function [20] we have calculated the expected phase change during time-of-flight to be less than  $\pi/10$  for our parameters. To evaluate the influence of density modulations on our measurements we have performed numerical simulations including the phase and density evolution. The inset in Fig. 3 compares a numerical result with Eq. (7). The excellent agreement demonstrates that this evolution can be neglected for our intensity correlation measurements and justifies the use of Eq. (7) to extract the phase correlation properties.

In conclusion, we have demonstrated a new interferometric method which allows us to measure the spatial correlation function of phase fluctuating BECs. First the second order correlation function was calculated and it was shown that this function can be measured using intensity correlations in the interference pattern. Our measurements were then compared with these results, confirming both, the expected functional form of the correlation function and the phase coherence length of the sample. We have confirmed that this technique is insensitive to fluctuations of the relative global phase during

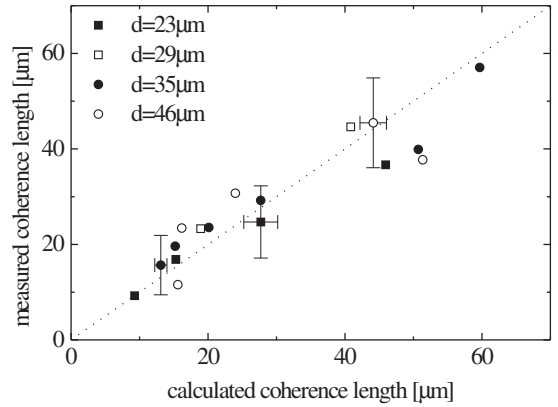


FIG. 4: Measured phase coherence length compared to the theoretically expected one given by Eq. (4). The dotted line  $f(x) = x$  is a guide to the eye. The error bars indicate statistical errors. Systematic uncertainties are 26% and 15% for the calculated and measured  $L_\phi$ , respectively.

the interferometric measurement sequence.

We thank L. Santos for valuable discussions and calculations on the expansion of phase fluctuating BECs. This work is supported by the *Deutsche Forschungsgemeinschaft* within the SFB 407.

---

\* hellweg@iqo.uni-hannover.de

- [1] M. R. Andrews et al., *Science* **275**, 637 (1997).
- [2] E. W. Hagley et al., *Phys. Rev. Lett.* **83**, 3112 (1999).
- [3] J. Stenger et al., *Phys. Rev. Lett.* **82**, 4569 (1999).
- [4] I. Bloch, T. W. Hänsch, and T. Esslinger, *Nature* **403**, 166 (2000).
- [5] D. S. Petrov, G. V. Shlyapnikov, and J. T. M. Walraven, *Phys. Rev. Lett.* **85**, 3745 (2000), and references therein.
- [6] D. S. Petrov, G. V. Shlyapnikov, and J. T. M. Walraven, *Phys. Rev. Lett.* **87**, 050404 (2001).
- [7] C. Mora and Y. Castin, cond-mat/0212523.
- [8] J. O. Andersen, U. Al Khawaja, and H. T. C. Stoof, *Phys. Rev. Lett.* **88**, 070407 (2002).
- [9] U. Al Khawaja et al., *Phys. Rev. A* **66**, 013615 (2002).
- [10] D. L. Luxat and A. Griffin, cond-mat/0212103.
- [11] S. Dettmer et al., *Phys. Rev. Lett.* **87**, 160406 (2001).
- [12] D. Hellweg et al., *Appl. Phys. B* **73**, 781 (2001).
- [13] H. Kreutzmann et al., *Appl. Phys. B* **76**, 165 (2003).
- [14] S. Richard et al., cond-mat/0303137.
- [15] F. Gerbier et al., cond-mat/0211094.
- [16] I. Shvarchuck et al., *Phys. Rev. Lett.* **89**, 270404 (2002).
- [17] R. Hanbury Brown and R. Q. Twiss, *Nature* **177**, 27 (1956).
- [18] R. Hanbury Brown and R. Q. Twiss, *Nature* **178**, 1046 (1956).
- [19] See e.g. M. O. Scully and M. S. Zubairy, *Quantum Optics* (Cambridge University Press, 1997).
- [20] More details will be given in L. Cacciapuoti et al., in preparation (2003).
- [21] J. E. Simsarian et al., *Phys. Rev. Lett.* **85**, 2040 (2000).
- [22] Y. Castin and R. Dum, *Phys. Rev. Lett.* **77**, 5315 (1996).

- [23] Yu. Kagan, E. L. Surkov, and G. V. Shlyapnikov, Phys. Rev. A **54**, 1753(R) (1996).
- [24] Y. Torii et al., Phys. Rev. A **61**, 041602(R) (2000).
- [25] After this time we do not observe any quadrupole oscillations; we measured the thermalization time of our condensates to be a few 100 ms.
- [26] The origin of the x-axis has been set to the center of the two overlapping clouds.
- [27] Compared to previous autocorrelation measurements with BECs [21] our signal is highly sensitive to such fluctuations because of the long  $\Delta t$  needed to reach a sufficient displacement.
- [28] Note that the measured frequency of the cosine is in good agreement with the prediction of  $\alpha$  and  $\beta$ .